

Carbon Gain and Allocation in Five Shade Intolerant *Pinus* Species

By

Yi Wang

Advisors: Dr. Sari Palmroth, Dr. Ram Oren, and Dr. Christopher A. Maier

December 7, 2021

Masters project submitted in partial fulfillment of the
requirements for the Master of Environmental Management and
the Master of Forestry concurrent degree in
the Nicholas School of the Environment of
Duke University

Executive Summary

As the largest genus among the gymnosperms, the genus of *Pinus* has a wide geographical range, occupies diverse ecological niches, and includes some of the most ecologically and economically valuable tree species. Pine plantations in the southeastern US provide about 16% of the industrial wood demand globally and make up about 28% of forest cover regionally. *Pinus virginiana* (Virginia pine), *Pinus echinata* (shortleaf pine), *Pinus taeda* (loblolly pine), *Pinus elliottii* (slash pine), and *Pinus palustris* (longleaf pine) are five of the most dominant shade-intolerant pine species in the southeast region. These five species have overlapping geographic ranges, tolerate poor soil conditions and low water availability conditions, and have relatively high volume growth rate. Among the five species, *P. virginiana* and *P. echinata* have the shortest needles of around 5-7 cm. *P. taeda* and *P. elliottii* have the intermediate needle length of around 15-22 cm, while *P. palustris* has the longest needles of around 30 cm.

Leaf traits, biomass allocation and volume growth rate of these species have been compared in previous studies, especially for *P. taeda*, *P. elliottii*, and *P. palustris* due to their ecological and economical values. Most of the established studies focused on the differences of aboveground growth rate within and among species in relation to different genotypes, climate and soil conditions, and management strategies. To compare the among species differences in biomass growth rate based on their physiology, morphology, and hydraulics related leaf traits, shoot and crown structure, and biomass allocation, we collected the data from an experimental site in Duke Forest and compared the performance of these five species when trees of the same age were grown under the same climate and soil conditions.

The overall objectives of this study were to explore the biomass allocation patterns, growth-related functional traits, and crown structure among species, to quantify the biomass growth rate and growth efficiency, to determine the costs and benefits of different leaf display strategies, and to provide additional information for specie-site selection and management in practice. In this study, we focused on the following questions:

1. What are the similarities and differences in biomass allocation patterns among species?
2. How do leaf functional traits and crown structure vary within and across species?

3. Why do *P. taeda* and *P. elliottii* have higher biomass growth rate and stem wood production than other species?

Our study revealed distinct differences in allometric relationships and biomass allocation patterns among the five species. Analysis of leaf functional traits and crown structure showed variation in the ability to support leaf area at a given leaf mass, branch mass, and sapwood area across species. Finally, the differences in total biomass and wood production among species reflected the combined effect of leaf area index and biomass allocation pattern. We found that, when growing in one environment, species with intermediate needle length (*P. taeda* and *P. elliottii*) were more efficient in biomass production and volume growth while balancing the investment in intercepting light and maintaining hydraulic system. The results of this study indicated that growth-related functional traits, combined with biomass allocation patterns that favor stem and aboveground production, make *P. taeda* and *P. elliottii* among the fastest growing conifers with high timber values, regionally and globally.

Contents

1	Introduction	4
2	Materials and Methods	6
2.1	Site description	6
2.2	Data collection and measurements	6
2.3	Data analysis	8
3	Results	11
3.1	Variation in total biomass, allometric models, and biomass allocation among species	11
3.2	Variation in leaf traits and crown structure among species	15
3.3	Variation in leaf and branch distribution patterns among species	18
3.4	Variation in leaf-to-sapwood area ratio among species	20
3.5	Variation in growth rate and growth efficiency among species	23
4	Discussion and Conclusion	24
4.1	Biomass allometry and allocation	25
4.2	Leaf functional traits and crown structure	26
4.3	Growth rate and growth efficiency	26
Reference		28
Appendix		31

1 Introduction

As the largest genus in gymnosperms, the genus *Pinus* includes more than 100 species with a wide geographic range, diverse ecological niches, and complicated evolutionary history (Keeley, 2012; Jin et al., 2021). Pine plantations in southern United States cover more than 80 million acres of land, make up about 28% of forest cover regionally, and provide about 16% of industrial wood supply globally (Wear and Greis, 2002, 2012; Fagan et al., 2018).

Four "southern pine" species from *Australes* subsection (Gaby, 1985), *Pinus echinata* (shortleaf pine), *Pinus taeda* (loblolly pine), *Pinus elliottii* (slash pine), *Pinus palustris* (longleaf pine), together with *Pinus virginiana* from *Contartae* subsection, are the five dominant pine species in southern region of United States. These five shade intolerant pine species have partially overlapping geographic ranges, tolerate poor soil conditions and low water availability conditions, and have relatively high volume growth rate ($< 10 \text{ m}^3 \text{ ha}^{-1} \text{ yr}^{-1}$ for *P. virginiana*, $> 10 \text{ m}^3 \text{ ha}^{-1} \text{ yr}^{-1}$ for the four other species) (Burns et al., 1990). Among the five species, *P. virginiana* and *P. echinata* have the shortest needles of around 5-7 cm. *P. taeda* and *P. elliottii* have the intermediate needle length of around 15-22 cm, while *P. palustris* has the longest needle of around 30 cm.

Leaf traits, biomass allocation and volume growth rate of these species have been compared in previous studies, especially for *P. taeda*, *P. elliottii*, and *P. palustris* due to their ecological and economical values. Most of the established studies focused on the differences of aboveground growth rate within and among species in relation to different genotypes, climate and soil conditions, and management strategies (Stearns-Smith et al., 1992; Chmura et al., 2007; Chmura and Tjoelker, 2008; Samuelson et al., 2012). However, the explanations of the among species differences in biomass growth rate based on their physiology, morphology, and hydraulics related leaf traits (e.g., leaf-to-sapwood area ratio), shoot and crown structure, and biomass allocation patterns under similar climate and soil conditions are still rare.

Leaf-to-sapwood area ratio ($A_l:A_s$), particularly, is critical to plant hydraulic balance and carbon allocation. Sapwood and heartwood are two different wood compartments in perennial stems with distinct functions. Sapwood is physiologically active, while heartwood contains no living cells (Bamber, 1976; Lehnebach et al., 2018). The allometric relationship between the sapwood

area and whole-tree leaf area was initially identified as Huber value (Huber, 1928; Waring et al., 1982; McDowell et al., 2002). This relationship was generalized as the pipe model (Shinozaki et al., 1964a,b), which suggested that the leaf-to-sapwood area ratio remains constant in every development stage of plant (Shinozaki et al., 1964a). With this widely used model, it is possible to estimate the leaf area of a tree from its sapwood area and tree-level $A_l:A_s$, and furthermore the leaf area of an entire stand (leaf area per unit ground area, i.e., leaf area index) within given basal area and a relationship between basal area and sapwood area (Waring et al., 1982; Oren et al., 1986).

While comparison of $A_l:A_s$ among species provides insight into potential differences in carbon allocation between photosynthesizing and water-conducting tissues, stand leaf area index (LAI) is a proxy for canopy light interception and thus potential carbon gain (Waring, 1983). When estimates of annual biomass production are available, further insight to carbon allocation can be gained through analyzing the components of production: LAI and growth efficiency, where growth efficiency is the annual (stem, aboveground or total biomass) growth per unit leaf area.

The overall objectives of this study were to compare the performance of these five pine species (at the same age and when grown on the same site) and (1) to explore the differences and similarities in the biomass allocation patterns, growth-related functional traits, and crown structure among species, (2) to quantify the biomass growth rate and growth efficiency based on the allometric relationships and leaf area estimate generated from the relationship between leaf area and conducting xylem, (3) to determine the cost and benefit of different leaf display strategies, and (4) to provide additional information for specie-site selection and management in practice. In this study, we focused on the following questions:

1. What are the similarities and differences in biomass allocation patterns among species?
2. How do leaf functional traits and crown structure vary within and across species?
3. Why do *P. taeda* and *P. elliottii* have higher biomass growth rate and stem wood production than other species?

2 Materials and Methods

2.1 Site description

The study was performed on trees from an experimental site in the Duke Forest, Durham, NC, with flat terrain and sandy loam soil of the Appling series. The mean annual temperature of the region is 15.5 °C with highest mean of 21.1 °C and lowest mean of 8.9 °C. The precipitation is evenly distributed throughout the year with annual precipitation of 1,145 mm (Wang et al., 2019).

One-year-old seedlings of the five southern pine species, *Pinus virginiana* (Virginia pine), *Pinus echinata* (shortleaf pine), *Pinus taeda* (loblolly pine), *Pinus elliottii* (slash pine), and *Pinus palustris* (longleaf pine), were planted in 32 m × 40 m plots with 4 m × 2 m spacing in 2011. *P. virginiana* seedlings were from Claridge Nursery, Goldsboro, NC. The seedlings of *P. echinata* and *P. elliottii* were from Flint River Nursery, Byromville, GA, and *P. taeda* seedlings of two mass controlled pollinated families representing broad and narrow crown ideotypes were from Supertree Nursery, Blenheim SC. *P. palustris* seedlings with various provenances across the southeastern US were from Longleaf Pine Regional Provenance/Progeny Trial, NC State University Cooperative Tree Improvement Program and USDA Forest Service, Raleigh, NC (Wang et al., 2019). Diameter at breast height (DBH) and total tree height (H) were measured annually, and at the end of growing season in 2020, the dominant height of the five species stands were: *P. virginiana* - 4.1 m, *P. echinata* - 4.0 m, *P. taeda* - 10.2 m, *P. elliottii* - 5.9 m, and *P. palustris* - 2.8 m.

2.2 Data collection and measurements

Data in this study were collected from 25 sample trees (five trees per species) in the experimental site. Trees with neighbors were selected across the DBH and height range of each species as sample trees (Figure 1). In addition to the destructive sampling, trees in the experimental site were measured annually to obtain the DBH and height data.

Biomass

Above-ground biomass (AGB) was measured based on destructive sampling between October 2019 and April 2020. Trees were partitioned into needle, branch, stem, cone, and epicormic branch components. All components were oven dried at 65 °C until constant weight was achieved and measured in laboratory (USDA Forest Service Laboratory, Research Triangle Park, NC).

Below-ground biomass (BGB) sampling was performed in June 2020. Coarse roots (>2mm in diameter) were sampled using a combination of excavation down to 100 cm in a central pit (1 m × 1 m) and four cores outside of the pit for each sample tree. Coarse roots were collected by sieving soil through 0.64 cm² mesh hardware screen. A backhoe was used to remove the entire taproot if necessary. Taproots and lateral roots were separated in the field. After pit excavation, two cores between trees on the row and two cores between rows were collected for each sample tree. A 15.25 cm auger was used to sample 0-20 and 20-40 cm depths followed by a 10.2 cm auger for the 40-100 cm depth. Root samples were then washed with de-ionized water, oven dried at 65 °C until constant weight was achieved, and weighed in laboratory.

Leaf traits and crown structure measurements

Diameter at breast height (DBH), total tree height, stem diameter at the base of live crown, height of live crown on the stem, total length of live crown were measured for each sample tree. In addition, each branch on the tree was measured to obtain its height on the stem and branch diameter.

Live crown of each tree was divided into five sections with equal crown length. Diameter and bark thickness at four directions (north, south, east, west) at the bottom stem of each crown section were then measured.

For each crown section, one representative sample branch was selected, and its total length and horizontal distance from stem to branch tip were measured. Sample branches were partitioned into branch segments, and branch segment order (primary, secondary, tertiary, quaternary) and age (needles from 2017, 2018, 2019) were then determined. Segment diameter, segment length, and oven-dry weight of wood and needles were also measured.

For leaf traits measurement, needle samples were collected from primary segments and secondary segments with tertiary and quaternary segments. Ten fascicles of needles in each age class from different segment orders were sampled for projected specific leaf area (SLA, $\text{cm}^2 \text{ g}^{-1}$) and needle length measurements. After needles were dried with paper towels, projected needle area (cm^2), needle angle ($^\circ$) and needle length (cm) were obtained from scanned image analysis software Image-J (National Institutes of Health, MD). Projected specific leaf area was calculated as the ratio of projected needle surface area to needle dry mass. The remaining stem, branches, needles, and cones in each crown section were separated, oven dried, and weighed.

2.3 Data analysis

SLA and leaf area estimate

Projected specific leaf area (SLA) values were estimated by mean SLA values of needle samples with same needle age and same segment order. For each crown section, SLA for needles in each age class was estimated from the mean SLA value of needle samples from the same age class in that crown section. Projected leaf area was then calculated as needle mass \times estimated SLA. Leaf-to-sapwood area ratio ($A_l:A_s$, $\text{m}^2 \text{ cm}^{-2}$) was calculated by the ratio between total projected leaf area and sapwood area.

Bark thickness correction

Ratio of sapwood area (inside bark) and stem cross-sectional area (outside bark) was calculated from the stem diameter and bark thickness measurement data at the bottom stem of each crown section. A second order polynomial regression relating the inside-outside bark area ratio and relative height within the crown was developed for each species. The sapwood area for each branch on the sample trees was then calculated based on its cross-sectional area and its relative height within the crown.

Lateral root scaling

Lateral root biomass was estimated based on the weight of collected root samples and statistical scaling methods described in Maier et al. (2021). Lateral root biomass for each tree was estimated separately in three concentric zones around each tree. Total lateral root biomass was then calculated by summing up the biomass values from each zone.

Roots in zone 1 was scaled using the lateral roots collected in the central pit as:

$$B_{lr1} = P \times (a_1/1) \quad (1)$$

where B_{lr1} is lateral root biomass (kg) in zone 1, P is lateral root biomass in the 1 m² pit (kg m⁻²), and a_1 is the area of zone 1 (1.57 m²). Roots collected from the four cores were used to estimate root biomass in zone 2 as:

$$B_{lr2} = T \times (a_2 - a_1) \quad (2)$$

where B_{lr2} is lateral root biomass (kg) in zone 2, T is lateral root biomass in the four 15.25 cm² coring trench (kg m⁻²), and a_2 is the area of zone 2 (7 m²). To estimate lateral root biomass in zone 3, we calculated the maximum root area (MRA, m²) for each tree to represent the DBH-derived root spread (Maier et al., 2021) as:

$$MRA = 106.15 \times D^{1.18} \quad (3)$$

where MRA is area (m²) occupied by roots, and D is stem diameter (m). Root biomass in zone 3 was estimated from roots collect from the trench as:

$$B_{lr3} = T \times (MRA - a_2) \times CF \quad (4)$$

where B_{lr3} is root biomass in zone 3 and CF (0.2399) is a correction factor to correct biomass attenuation along the distance between the edge of zone 2 to the edge of zone 3. This correction factor was derived from a normalized decay function quantifying the relationship between root cross-sectional area, which is proportional to root biomass, and distance from an inflection point, where roots transit from mechanical support and transport function to only transport (~1.3 m from stem, Oren, unpublished data).

Total lateral root biomass was then estimated as:

$$B_{lr} = B_{lr1} + B_{lr2} + B_{lr3} \quad (5)$$

Allometric models

Allometric equations were developed for each species to model biomass using DBH and height as predicting variables. Species-specific allometric equations were derived from the data collected from the 25 sample trees. Equations for total biomass, total above-ground biomass (AGB), total below-ground biomass (BGB), live foliage biomass, branch biomass, and stem biomass (outside bark) were generated separately.

Biomass Growth Rate and Growth Efficiency

Leaf area index (LAI, $\text{m}^2 \text{ m}^{-2}$) was calculated based on the linear relationship developed between the crown base sapwood area and total leaf area. DBH data from trees with continuous measurements were corrected by specie specific bark thickness value to get the sapwood area, and then converted to total leaf area. LAI was then obtained by scaling the total leaf area in the stand to leaf area per unit of ground area using the count of trees with continuous measurements and the spacing between trees.

The standing biomass of each year was calculated based on the species-specific biomass allometric models and tree size data (DBH and height) from continuous measurements in the experimental stand between 2018 and 2021. Biomass growth rate ($\text{kg yr}^{-1} \text{ m}^{-2}$) was calculated as the biomass gain per year per unit of ground area. Growth efficiency (GE, $\text{kg yr}^{-1} \text{ m}^{-2} \text{ LAI}$) was generated for each species by dividing biomass growth rate by LAI to represent the amount of annual production per unit of leaf area. Allometric models for total biomass and stem biomass were used separately to generate the total growth rate/efficiency and stem growth rate/efficiency.

Statistical analysis

The effects of species on projected specific leaf area (SLA), needle length, crown ratio, leaf-to-sapwood area ratio ($A_l:A_s$), biomass allocation by compartment were evaluated by one-way analysis of variance (ANOVA). Fisher's least significant difference test was used to perform the multi-comparisons to identify the species groups with significant differences in those variables.

Linear regression models were used to evaluate relationships among leaf area, leaf mass, branch sapwood area, and crown base sapwood area, also the similarities and differences of these relationships across species. For regressions at the sample branch level, intercepts were set to 0. Analysis of covariance (ANCOVA) and multiple comparisons were used to test if slopes ($A_l:A_s$) of these relationships vary significantly from species to species.

Multiple curve fitting methods (linear regression, second order polynomial regression, Modified Akima piecewise cubic Hermite interpolation) were used to visualize the change of needle length, SLA, $A_l:A_s$, leaf area, leaf mass along the relative height within the crown. Leaf area and leaf mass were displayed as relative values to total leaf area and leaf mass.

Probability levels of $P < 0.05$ and $P < 0.10$ were used to determine the significance and tendency of a relationship respectively. All analyses and curve fitting were performed in MATLAB R2020b (version 9.9.0).

3 Results

3.1 Variation in total biomass, allometric models, and biomass allocation among species

The five *Pinus* species showed distinct difference in DBH and height after 10 years of growth (Figure 1). Across five *Pinus* species, total biomass ranged from 16.49 ± 4.00 kg in *P. echinata* to 43.05 ± 7.47 kg in *P. taeda* (Table 1). *P. taeda* had the highest values in biomass by compartments except for lateral root (Table S1). For the ratio between below-ground biomass and above-ground biomass (BGB: AGB), the difference among species was significant ($n = 5$ per species, $P = 0.0014$). Despite having the lowest total biomass, *P. echinata* had the highest BGB: AGB ratio of 0.40 ± 0.05 .

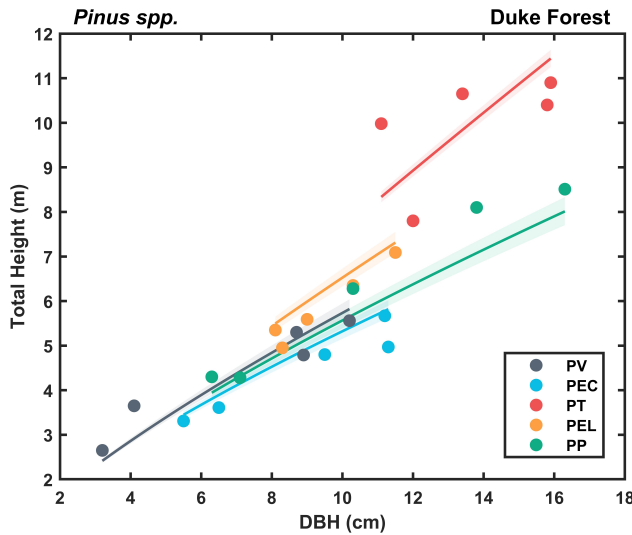


Figure 1: Relationships between DBH and total tree height of five *Pinus* species. Points represent the data from 25 sample trees. Lines represent linear regression models with logarithmic transformations of DBH and height data (within the size range of 25 sample trees) collected from the experimental stand from 2018 to 2021. PV: *Pinus virginiana*; PEC: *Pinus echinata*; PT: *Pinus taeda*; PEL: *Pinus elliottii*; PP: *Pinus palustris*

Table 1: Biomass in five *Pinus* species (n = 5 per species, mean \pm SE, range)

Species	Code	Total Biomass (kg)	Aboveground Biomass (kg)	Belowground Biomass (kg)	BGB:AGB
<i>Pinus virginiana</i>	PV	17.45 \pm 6.03	13.54 \pm 4.70	3.92 \pm 1.34	0.28 \pm 0.01
		3.17 – 32.73	2.51 – 25.89	0.66 – 6.84	0.26 – 0.33
<i>Pinus echinata</i>	PEC	16.49 \pm 4.00	12.02 \pm 3.10	4.47 \pm 0.95	0.40 \pm 0.05
		5.44 – 24.86	3.98 – 18.47	1.46 – 6.39	0.31 – 0.57
<i>Pinus taeda</i>	PT	43.05 \pm 7.47	34.70 \pm 6.42	8.36 \pm 1.20	0.25 \pm 0.03
		25.47 – 62.82	20.74 – 50.92	4.73 – 11.89	0.20 – 0.39
<i>Pinus elliottii</i>	PEL	17.75 \pm 4.60	14.66 \pm 3.78	3.09 \pm 0.84	0.21 \pm 0.02
		9.53 – 34.87	8.16 – 28.90	1.37 – 5.97	0.17 – 0.26
<i>Pinus palustris</i>	PP	31.04 \pm 11.28	23.76 \pm 8.83	7.28 \pm 2.46	0.33 \pm 0.02
		7.14 – 64.88	5.06 – 50.77	2.08 – 14.11	0.28 – 0.41

The coefficient estimates for the non-linear regression models to predict total biomass, total above-ground biomass (AGB), total below-ground biomass (BGB), live foliage biomass, branch biomass, and stem biomass (outside bark) are listed in Table 2 (Total Biomass) and Table S1-S5

(AGB, BGB, stem, branch, and foliage).

Table 2: Coefficient estimates and fit statistics of total biomass allometric equation in five *Pinus* species ($y = a(DBH^2 * Height)^b$)

Species	Code	DBH (cm)	Height (m)	a	SE	b	SE	R ²	RMSE
<i>Pinus virginiana</i>	PV	3.2 – 10.2	2.65 – 5.56	0.131272	0.068745	0.870013	0.085231	0.991121	1.269542
<i>Pinus echinata</i>	PEC	5.5 – 11.3	3.31 – 5.67	0.264198	0.146209	0.696907	0.087491	0.968868	1.577751
<i>Pinus taeda</i>	PT	11.1 – 15.9	7.80 – 10.90	0.023598	0.018053	0.992884	0.098985	0.969932	2.897527
<i>Pinus elliottii</i>	PEL	8.1 – 11.5	4.95 – 7.09	0.006326	0.007529	1.252947	0.180046	0.933403	2.654537
<i>Pinus palustris</i>	PP	6.3 – 16.3	4.28 – 8.51	0.122028	0.023329	0.814018	0.025598	0.998327	1.032124

The patterns of biomass allocation to different compartments (Figures 2 and 3) varied significantly among species with P = 0.0010 for foliage, P = 0.0016 for taproot, and P < 0.0001 for branch, stem, and lateral root. *P. virginiana* had the highest percentage of branch biomass (Figure 2a), and *P. echinata* had the highest percentage of lateral root biomass (Figure 2b). *P. taeda* had the highest proportion of total biomass allocated to stem and taproot, but lowest proportion to foliage compared to other species (Figure 2c).

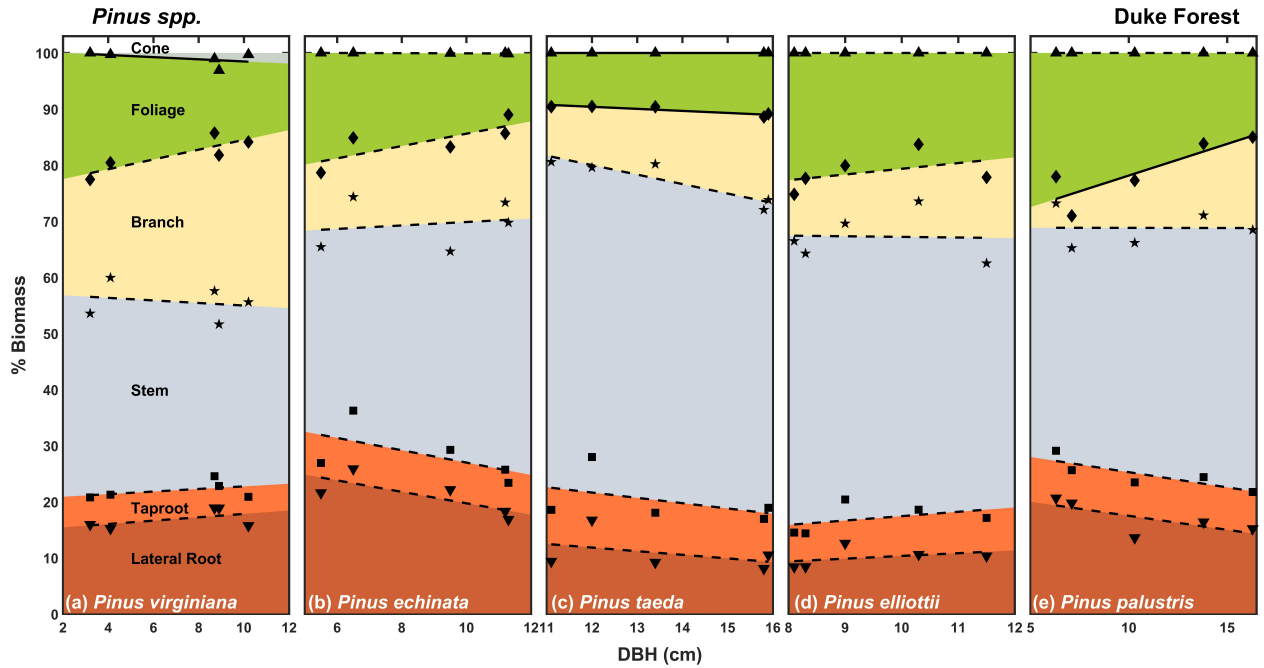


Figure 2: Relationships between DBH and biomass allocation patterns of five *Pinus* species. Points represent the cumulative percentage of biomass from 25 sample trees. Lines represent linear regression models of DBH and cumulative percentage of biomass, with solid and dotted lines representing regressions of DBH and biomass percentage by compartments with $P < 0.05$ and $P > 0.05$, respectively.

Biomass allocation patterns were also related to the size of the trees (Figure 3). For the two species with closed canopy, *P. virginiana* and *P. taeda*, the proportion of foliage biomass of the total biomass had significant linear relationships with DBH (Figure 3a, Table S6, $P = 0.0372$ and 0.0371 respectively). With increasing DBH, percentage of foliage biomass decreased for *P. virginiana* while increased for *P. taeda*. Percentage of foliage biomass for *P. palustris* also had a tendency to decrease with DBH ($P = 0.0654$). The proportion for branch biomass increased with DBH for all species (Figure 3b), with significant relationships for *P. taeda* and *P. palustris* ($P = 0.0271$ and 0.0024 respectively) and a tendency for *P. virginiana* ($P = 0.0523$). The relationships between DBH and percentage of biomass for other compartments were not significant (Table S8-S11, minimum $P = 0.0745$).

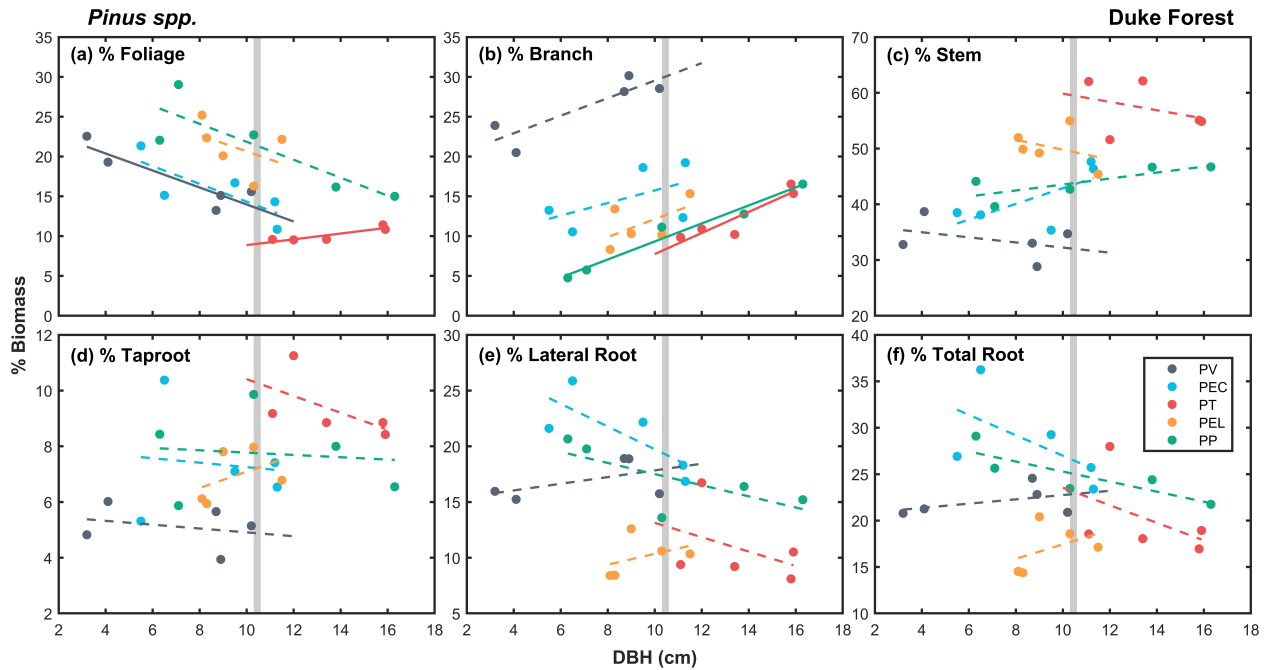


Figure 3: Relationships between diameter at breast height (DBH) and percentage of total biomass allocated to (a) foliage, (b) branch, (c) stem, (d) taproot, (e) lateral root, (f) total root biomass among five *Pinus* species. Points represent the biomass percentage of each compartment from 25 sample trees. Lines represent species-specific linear regression models between DBH and percentage of biomass for each compartment, with solid and dotted lines representing regressions with $P < 0.05$ and $P > 0.05$, respectively. The gray vertical lines intersect the relationship at a DBH = 10.5 cm, close to a diameter found in all species, allowing a comparison at a similar diameter. PV: *Pinus virginiana*; PEC: *Pinus echinata*; PT: *Pinus taeda*; PEL: *Pinus elliottii*; PP: *Pinus palustris*

3.2 Variation in leaf traits and crown structure among species

The five species showed both similarities and differences in leaf traits and crown structure (Table 3). Leaf-to-sapwood area ratio ($A_l:A_s$, $\text{m}^2 \text{ cm}^{-2}$) was not significantly different among five species, indicating similar amount of leaf area generated with same area of conducting xylem. Crown ratio showed distinctive overall crown structure among five species. *P. echinata* and *P. taeda* were the two species with significantly lower crown ratio ($P = 0.0100$), representing the higher starting point of living crown within the total tree height compared to three other species.

Needle length varied significantly across five species ($P < 0.0001$), from 4.53 ± 0.22 cm in *P. virginiana* to 25.07 ± 1.03 in *P. palustris*. The variation of needle length at different heights in the crown showed similar pattern among the five species (Figure S1). Compared to the bottom of the crown, the difference between minimum and maximum needle length at the tree top was relatively small.

Table 3: Leaf functional traits and crown ratio in five *Pinus* species (n = 5 per species, mean \pm SE, range)

Species	Code	Needle Length (cm)	Projected SLA ($\text{cm}^2 \text{ g}^{-1}$)	Al:As ($\text{m}^2 \text{ cm}^{-2}$)	Crown Ratio
<i>Pinus virginiana</i>	PV	4.53 ± 0.22	36.93 ± 1.61	0.20 ± 0.02	0.82 ± 0.03
		$1.91 - 8.32$	$33.61 - 42.19$	$0.16 - 0.25$	$0.75 - 0.88$
<i>Pinus echinata</i>	PEC	7.02 ± 0.19	39.16 ± 1.06	0.21 ± 0.03	0.72 ± 0.03
		$2.55 - 10.66$	$35.37 - 41.69$	$0.13 - 0.30$	$0.65 - 0.80$
<i>Pinus taeda</i>	PT	13.11 ± 0.38	44.45 ± 0.99	0.20 ± 0.01	0.70 ± 0.02
		$5.70 - 21.20$	$40.77 - 46.61$	$0.17 - 0.25$	$0.65 - 0.77$
<i>Pinus elliottii</i>	PEL	17.42 ± 0.63	35.02 ± 0.93	0.20 ± 0.04	0.82 ± 0.04
		$6.99 - 27.58$	$32.56 - 37.86$	$0.11 - 0.32$	$0.72 - 0.92$
<i>Pinus palustris</i>	PP	25.07 ± 1.03	36.74 ± 1.52	0.24 ± 0.03	0.81 ± 0.03
		$13.80 - 35.83$	$34.64 - 42.67$	$0.18 - 0.33$	$0.74 - 0.89$
P value		< 0.0001	0.0004	0.73	0.01

Specific leaf area (SLA, projected, $\text{cm}^2 \text{ g}^{-1}$) also varied among species ($P = 0.0004$). *P. taeda* had the highest specific leaf area among all other species (Figure 4), indicating the ability to generate higher leaf area for the same amount of biomass invested in leaves. Within each species group, needles from 2018 had significantly lower SLA than needle from 2019 (maximum $P = 0.0271$).

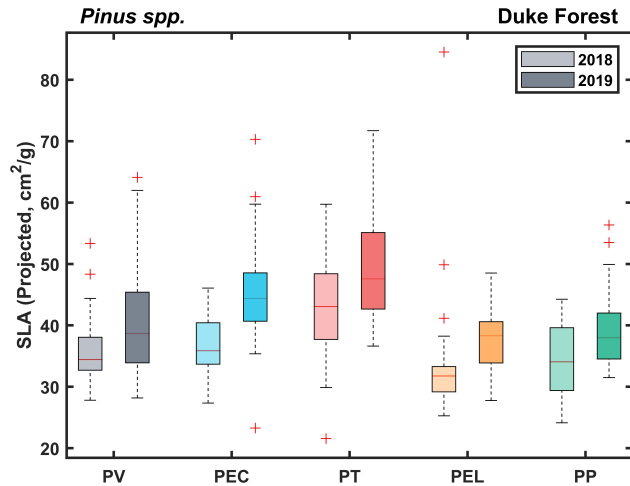


Figure 4: Variation of projected specific leaf area (SLA, $\text{cm}^2 \text{ g}^{-1}$) among species and age groups. Lighter color bars represent needles from 2018, and darker color bars represent needles from 2019. PV: *Pinus virginiana*; PEC: *Pinus echinata*; PT: *Pinus taeda*; PEL: *Pinus elliottii*; PP: *Pinus palustris*

The patterns of SLA change within the crown were different between species which closed their canopy at harvest time and those that remained more open (Figure 5). As two closed-canopy species, SLA for *P. virginiana* and *P. taeda* showed decreasing relationships with relative crown height ($P = 0.0215$ and 0.0057 respectively). SLA was highest at the bottom of the crown (Figure 5a), suggesting acclimation of leaves to shaded light condition in the canopies of these two species. While there were no clear patterns of SLA changes within the crown for other three species, maximum SLA values were generally achieved in the middle of the crown (Figure 5b).

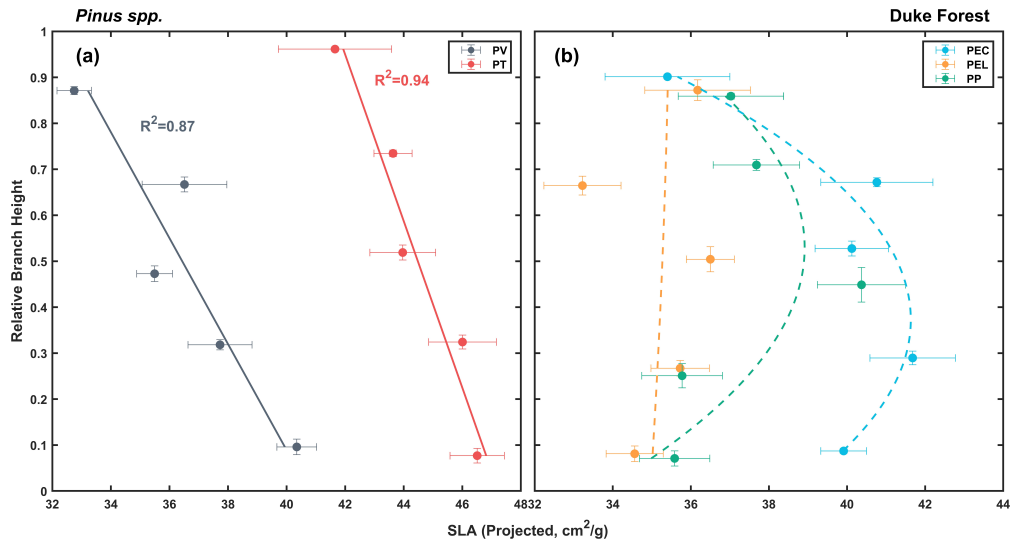


Figure 5: Relationships between projected specific leaf area (SLA, $\text{cm}^2 \text{ g}^{-1}$) and relative branch height within the live crown for (a) closed canopy species, (b) open canopy species. Points represent species means at each live crown section and error bars represent standard errors of the means ($n = 5$). Line represent species-specific models between SLA and relative branch height, with solid and dotted lines representing linear regressions and second order polynomial, respectively. Dotted lines are intended to guide the eye only. PV: *Pinus virginiana*; PEC: *Pinus echinata*; PT: *Pinus taeda*; PEL: *Pinus elliottii*; PP: *Pinus palustris*

3.3 Variation in leaf and branch distribution patterns among species

Leaf and branch mass distribution within the crown presented different patterns among species (Figure 6). *P. taeda* and *P. elliottii* had more leaf and branch mass allocated to the middle of the crown, while other species like *P. virginiana* had more leaf and branch mass toward the bottom of the crown.

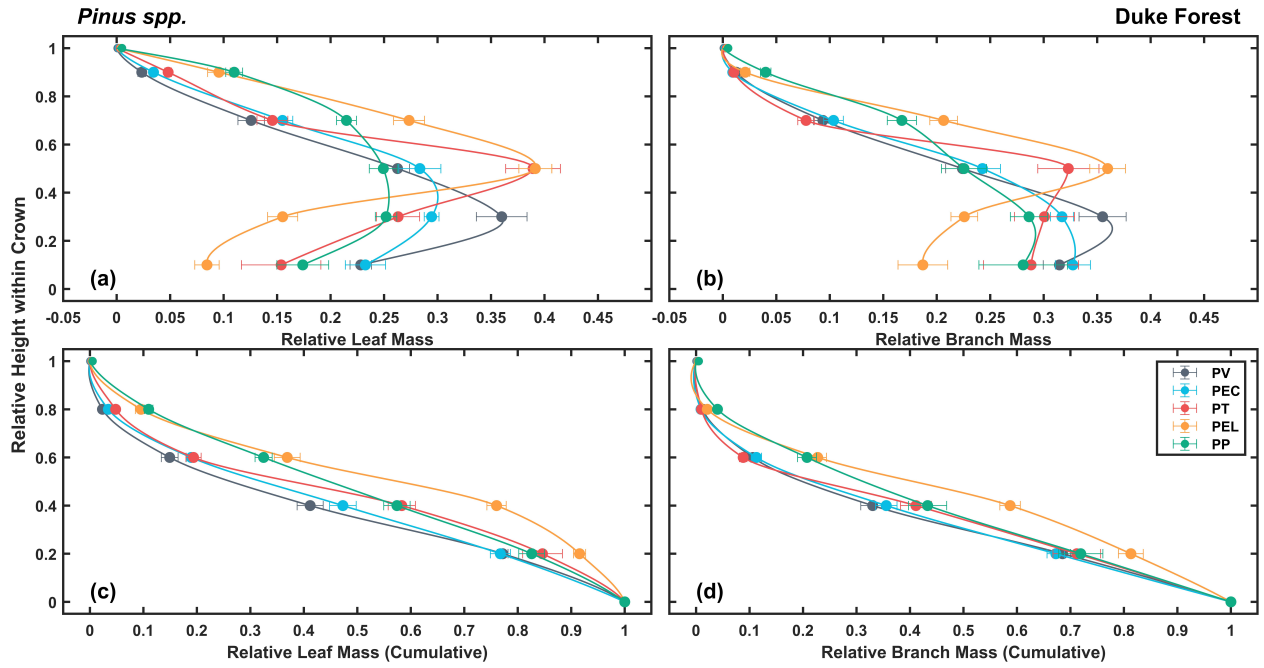


Figure 6: Relationships between (a) relative leaf mass, (b) relative branch mass, (c) relative leaf mass (cumulative), (d) relative branch mass (cumulative) and relative height within the live crown. Points represent species means at each live crown section and error bars represent standard errors of the means ($n = 5$). Lines represent the fits from Modified Akima piecewise cubic Hermite interpolation. Lines are intended to guide the eye only. PV: *Pinus virginiana*; PEC: *Pinus echinata*; PT: *Pinus taeda*; PEL: *Pinus elliottii*; PP: *Pinus palustris*

Leaf area distribution pattern (Figure 7) was different among species similarly to the leaf and branch mass distribution. *P. taeda* had significantly larger leaf area in the middle of the crown (Figure 7a). Despite having the highest number of branches compared to other species (Figure 7b), *P. virginiana* did not achieve highest total leaf area. Compared to the relatively even distribution pattern of leaf area in other species, *P. taeda* and *P. elliottii* had the highest leaf area per branch in the middle of the crown (Figure 7c).

The ratio between leaf area and branch mass indicated the balance between leaf area and the amount of supporting materials on each branch (Figure 7d). The relationships between leaf-area-to-branch-mass ratio and relative height within crown were significant for all five species (maximum $P = 0.0164$). The ratio increased from the bottom to the top of the crowns. The order of this ratio was similar to the order of needle length across species. *P. virginiana* had the lowest

leaf-area-to-branch-mass ratio, i.e., a large amount of biomass was invested in branches compared to the supported leaf area. The ratio was the highest in *P. palustris*, which indicated its ability to support large amount of leaf area per unit of biomass allocated to branch.

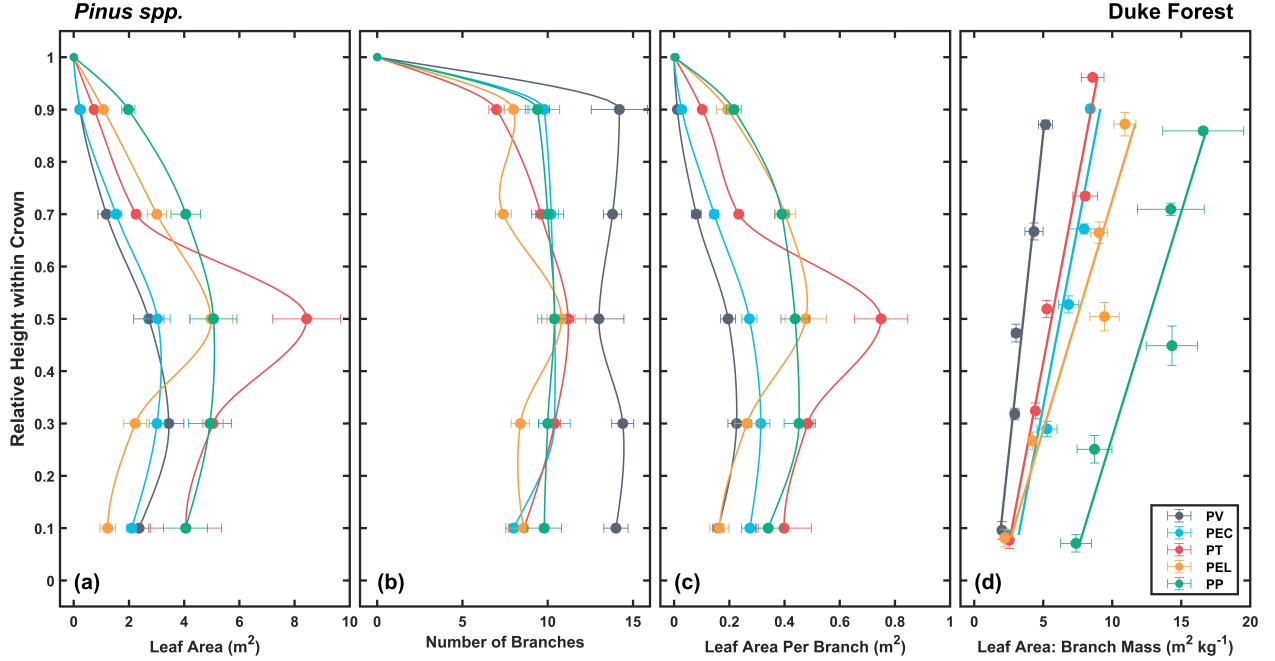


Figure 7: Relationships between (a) leaf area (m^2), (b) number of branches, (c) leaf area (m^2) per branch, (d) leaf-area-to-branch-mass ratio ($\text{m}^2 \text{ kg}^{-1}$), and relative height within the live crown. Points represent species means at each live crown section and error bars represent standard errors of the means ($n = 5$). Lines represent the fits from Modified Akima piecewise cubic Hermite interpolation. Lines are intended to guide the eye only. PV: *Pinus virginiana*; PEC: *Pinus echinata*; PT: *Pinus taeda*; PEL: *Pinus elliottii*; PP: *Pinus palustris*

3.4 Variation in leaf-to-sapwood area ratio among species

Branch leaf area was positively correlated with branch sapwood area (Figure 8a) for all five species (intercept was set to 0, $P < 0.0001$, $n = 25$ for each species). The slope of the regression between branch leaf area and branch sapwood area represented the leaf-to-sapwood area ratio of the branch (Table S12). The slope varied from 0.11 in *P. virginiana* to 0.22 in *P. elliottii*. Analysis of covariance (ANCOVA) showed significant difference of the slope among species ($P < 0.0001$). Multiple comparisons indicated significant groupings among species of the relationships between branch

leaf area and branch sapwood area. Two species with shorter needle, *P. virginiana* and *P. echinata* had similar slopes ($P = 0.6087$), which were significantly lower than the slopes in other three species. This difference indicated the difference in leaf area supported by a unit of conducting xylem. *P. taeda* and *P. elliottii* had the highest branch leaf-to-sapwood area ratio, which allowed the two species to have higher leaf area with the same amount of conducting xylem on the branch.

Branch leaf mass was also positively correlated with branch sapwood area (Figure 8b) for all five species (intercept = 0, $P < 0.0001$, $n = 25$ for each species). The slope of the regression also varied significantly ($P < 0.0001$) from 0.03 in *P. virginiana* and *P. echinata*, to 0.06 in *P. elliottii*. Unlike the relationship between branch leaf area and branch sapwood area, *P. taeda* had an intermediate ratio between branch leaf mass and branch sapwood area, while *P. elliottii* and *P. palustris* had higher branch leaf mass supported by the amount of branch conduced xylem.

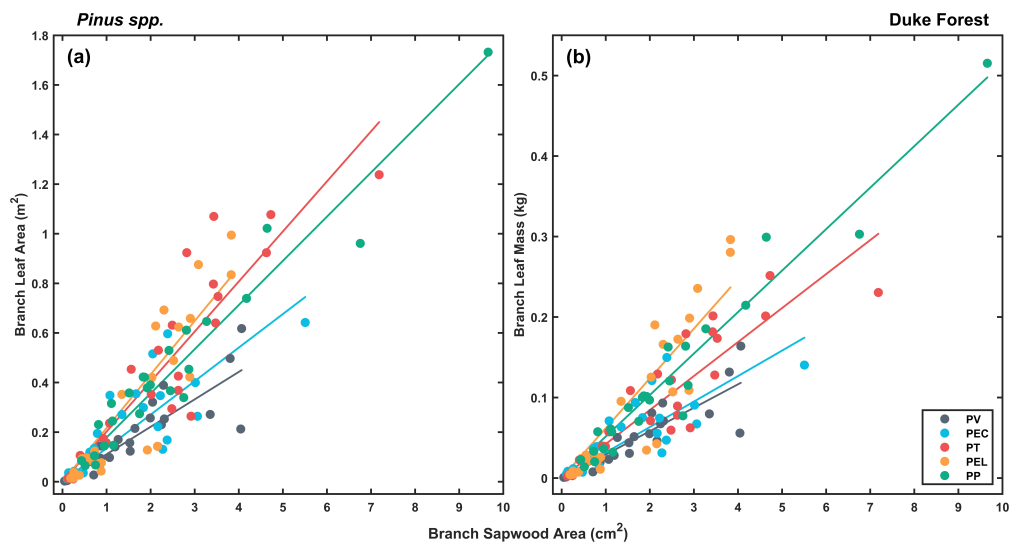


Figure 8: Relationships between branch sapwood area and (a) branch leaf area (m^2), (b) branch leaf mass (kg) among five *Pinus* species. Points represent sample branches ($n = 25$ per species), and lines represent the linear regression models with intercept set to 0. PV: *Pinus virginiana*; PEC: *Pinus echinata*; PT: *Pinus taeda*; PEL: *Pinus elliottii*; PP: *Pinus palustris*

The leaf-to-sapwood area ratio of the branch showed similar pattern within the crown across species (Figure 9). The ratio was highest in the middle of the crown for all five species. Overall, *P. taeda* and *P. elliottii* had the highest ratio compared to other species, providing more branch leaf area with the same branch sapwood ratio.

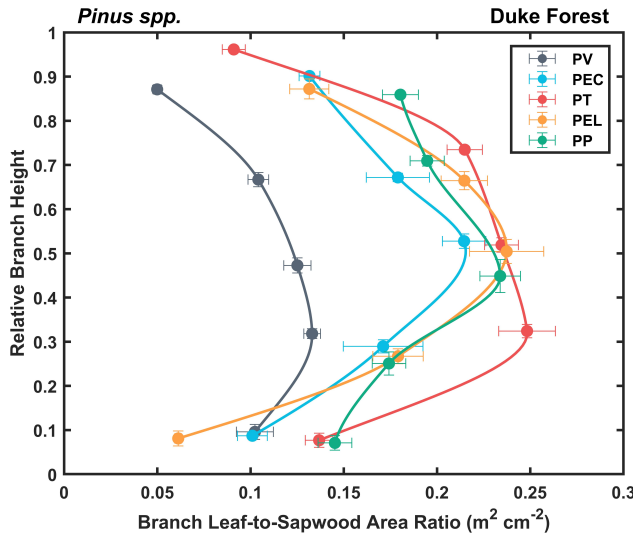


Figure 9: Relationships between branch leaf-to-sapwood area ratio ($A_l:A_s$, $\text{m}^2 \text{ cm}^{-2}$) and relative branch height within the live crown. Points represent species means at each live crown section and error bars represent standard errors of the means ($n = 5$). Lines represent the fits from Modified Akima piecewise cubic Hermite interpolation. Lines are intended to guide the eye only. PV: *Pinus virginiana*; PEC: *Pinus echinata*; PT: *Pinus taeda*; PEL: *Pinus elliottii*; PP: *Pinus palustris*

At the tree level, total leaf area, total leaf mass, and total branch sapwood area were all closely related to crown base sapwood area (Figure 10). The linear relationships between total leaf area and crown base sapwood area were not significantly different among species (Table S14-S16; minimum $P = 0.7135$) and the variation could be described with one regression line (Figure 10a, $R^2 = 0.83$, $P < 0.0001$). The relationship between total leaf mass and crown base sapwood area also suggested that, across all five species, the same amount of leaf mass was supported by a unit conducting xylem (Figure 10b, $R^2 = 0.73$, $P < 0.0001$). A strong linear relationship was also found between the area of conducting xylem at the base of live crown and the cumulative area of branch conducting xylem within the crown (Figure 10c, $R^2 = 0.78$, $P < 0.0001$). The slope of this single line had a 95% confidence interval of 1.09 to 1.70, indicating the ratio between total branch sapwood area and crown base sapwood area was significantly larger than 1 for these five species. The three general regression models all had an intercept not different from zero (minimum $P = 0.2268$).

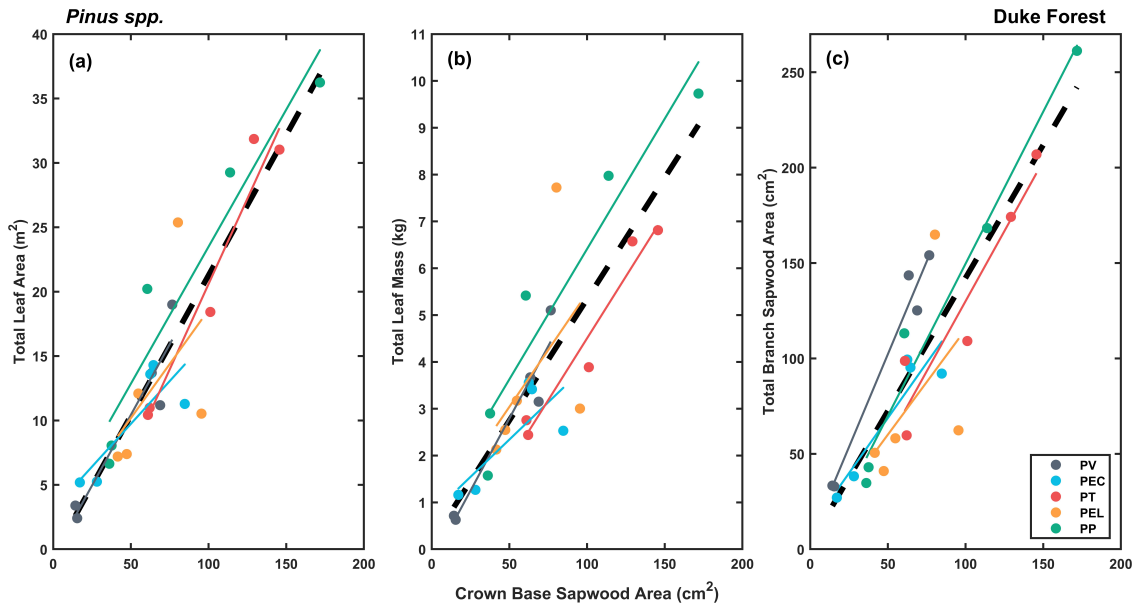


Figure 10: Relationships between sapwood area at live crown base and (a) total leaf area (m^2), (b) total leaf mass (kg), and (c) total branch sapwood area (cm^2) among five *Pinus* species. Points represent sample trees ($n = 5$ per species). Solid lines represent species-specific linear regression models. Thick dotted black lines represent general model for all five species. PV: *Pinus virginiana*; PEC: *Pinus echinata*; PT: *Pinus taeda*; PEL: *Pinus elliottii*; PP: *Pinus palustris*

3.5 Variation in growth rate and growth efficiency among species

The total biomass growth rate ($\text{kg yr}^{-1} \text{ m}^{-2}$) of the five species was positively related to the leaf area index (LAI, $\text{m}^2 \text{ m}^{-2}$) (Figure 11a, $R^2 = 0.99$, $P < 0.0001$) and varied from $0.33 \text{ kg yr}^{-1} \text{ m}^{-2}$ with LAI of $0.19 \text{ m}^2 \text{ m}^{-2}$ in *P. palustris* to $2.63 \text{ kg yr}^{-1} \text{ m}^{-2}$ with LAI of $1.54 \text{ m}^2 \text{ m}^{-2}$ in *P. taeda*. The total growth efficiency among the five species ranged from $1.36 \text{ kg yr}^{-1} \text{ m}^{-2}$ LAI in *P. virginiana* to $1.78 \text{ kg yr}^{-1} \text{ m}^{-2}$ LAI in *P. elliottii* (Figure 11b). The growth rate of stem wood was also strongly related with the leaf area index (Figure 11c, $R^2 = 0.98$, $P = 0.0008$). The stem wood growth efficiency was highest at the species with intermediate needle length (Figure 11d), indicating the ability to generate more stem wood production at a given leaf area for *P. taeda* and *P. elliottii*.

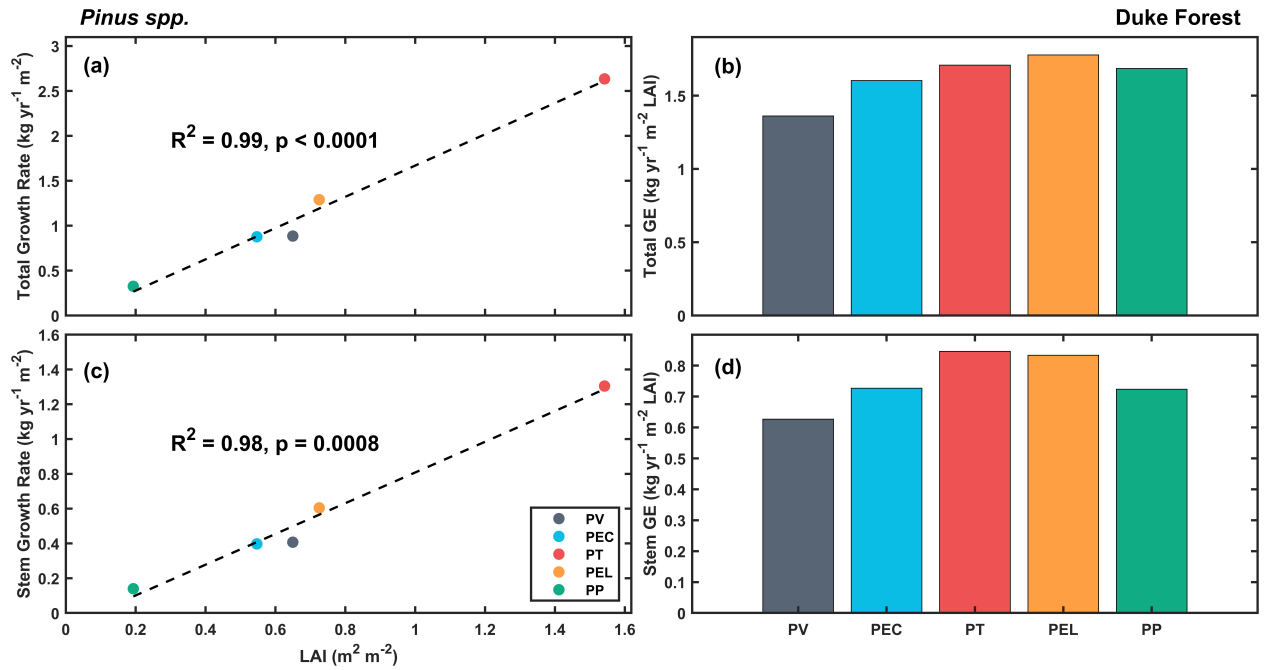


Figure 11: Relationships of (a) leaf area index (LAI, $\text{m}^2 \text{m}^{-2}$) and total growth rate ($\text{kg yr}^{-1} \text{m}^{-2}$), (b) sapwood area at live crown base and (a) total leaf area (m^2), (b) total growth efficiency ($\text{kg yr}^{-1} \text{m}^{-2} \text{LAI}$) among species, (c) leaf area index (LAI, $\text{m}^2 \text{m}^{-2}$) and stem growth rate ($\text{kg yr}^{-1} \text{m}^{-2}$), (d) stem growth efficiency ($\text{kg yr}^{-1} \text{m}^{-2} \text{LAI}$) among species. Points and bars represent five species. PV: *Pinus virginiana*; PEC: *Pinus echinata*; PT: *Pinus taeda*; PEL: *Pinus elliottii*; PP: *Pinus palustris*

4 Discussion and Conclusion

Our study first demonstrated the differences in biomass allometric relationships and biomass allocation patterns among the five shade intolerant *Pinus* species (Table 2, Table S1-S11, Figure 2-3). Analysis of leaf functional traits and crown structure showed variation in the ability to support different amounts of leaf area at a given leaf mass, branch mass, and sapwood area across species (Figure 4, 7, 8). Finally, the difference in biomass growth and wood production among species was the combined effect of leaf area index and allocation pattern (Figure 11). Our results suggested that when growing in one environment, species with intermediate needle length (*P. taeda* and *P. elliottii*) were more efficient in biomass production and volume growth while balancing the

investment in intercepting the light and maintaining the hydraulic system.

4.1 Biomass allometry and allocation

The biomass allometric models developed in this study covered a relatively wide range of trees in these five species with DBH less than 5 cm to more than 15 cm (Table 2). The allometric equations were also fit using the data from each compartment (Table S1-S5), which allowed further analysis of growth and allocation patterns of the five species, especially in the early stage (around 10 years) of tree growth. Compared to functions reported by Gonzalez-Benecke et al. (2014), the new set of relationships here focused on the tree growing under similar climate and soil condition, which provided more direct comparison for species selection decision at a given site.

Biomass allocation patterns revealed the different strategies across species in early stage of growth (Figure 2). *P. virginiana* invested more than 20% of its total biomass into branches, which corresponded to its crown shape. *P. echinata* on the other hand, invested almost 30% of its total biomass to root system, especially to lateral roots, which may benefit its nutrient uptake capacity and productivity under drought condition. Two species with intermediate needle length, *P. taeda* and *P. elliottii* allocated about 50% of total biomass to the stem, indicating the allocation pattern that favors the production of stem wood compared to other species. *P. palustris* showed the tendency to invest more biomass to its leaf and root, instead of developing branches and stem volume.

For the two species that had reached canopy closure, *P. virginiana* and *P. taeda*, the percentage of foliage biomass was strongly related to their tree size (Figure 3a, Table S6). However, with increasing DBH, percentage foliage biomass changed to contrasting pattern between these two species. For *P. virginiana*, a decreasing trend could be related to the balance between light interception and maintenance of the branch structure with increased tree size. *P. taeda*, on the other hand, showed the ability to produce more foliage mass with increasing DBH, which reflect the competitive advantage of larger individuals in terms of light capturing in a closed canopy.

4.2 Leaf functional traits and crown structure

The changing patterns of specific leaf area (Figure 5), leaf and branch distribution (Figure 6-7), and leaf-to-sapwood area ratio (Figure 9) within the living crown showed both similarities and differences across species. However, most of the patterns were visualized by certain data interpolation models to guide the eyes and perform cross species comparison; quantitative analyses of leaf traits patterns and crown structure within species are still needed.

Despite having the lowest percentage of biomass allocated to foliage, *P. taeda* was able to generate higher leaf area due to its higher specific leaf area (SLA, Figure 4), intermediate leaf-area-to-branch-mass ratio (Figure 7d), and higher branch leaf-to-sapwood area ratio ($A_l:A_s$, Figure 8a, Figure 9). It is plausible that, the intermediate leaf-area-to-branch-mass ratio found in both *P. taeda* and *P. elliottii* reflects a crown structure with the least amount of mutual shading and highest light interception. Furthermore, higher leaf-to-sapwood area ratio, as an indication of the capacity to support higher leaf area at a given conducting xylem area, allowed *P. taeda* and *P. elliottii* to generate more light intercepting area at the branch level.

4.3 Growth rate and growth efficiency

Across species, the variation in the stand biomass growth rate was largely explained by the difference in leaf area index (LAI) (Figure 11). With the two highest LAI values of *P. taeda* and *P. elliottii*, the total biomass growth rate (Figure 11a) and the annual stem wood production rate (Figure 11c) were the highest among all five species. Since all five species in this study are shade intolerant, the increasing mutual shading caused by higher LAI may decrease growth efficiency at certain stage of growth within species (Waring, 1983).

However, at a given sapwood area the five species showed no significant difference in total leaf area, total leaf mass, and total branch sapwood area (Figure 10). When the total biomass growth and stem wood production were scaled at per unit of LAI basis (Figure 11b and Figure 11d), the two species with intermediate needle length, *P. taeda* and *P. elliottii* were still able to maintain the highest growth efficiency compared to other species. Thus, despite having a higher leaf area index, these two species were able to produce more annual growth and stem wood production per unit

leaf area.

The intermediate needle length of *P. taeda* and *P. elliottii* may be associated with shoot and crown architecture that are better at capturing light at a given leaf area. In fact, as an indication of the shoot clumping factor of each species, the spherical mean of the shoot silhouette-to-total leaf area ratio (\overline{STAR}) showed the similar pattern as growth efficiency with maximizing at the intermediate needle length (Thérézien et al., 2007). This key factor of canopy light interception capacity, together with other hydraulic related traits (e.g. hydraulic conductivity), allow these two species with intermediate needle length to keep stomata open and perform photosynthesis more efficiently than other species. The results of this study indicated that these growth-related functional traits, combined with biomass allocation patterns that favor stem and aboveground production, make *P. taeda* and *P. elliottii* among the fastest growing conifers with high timber values, regionally and globally.

References

- R. Bamber. Heartwood, its function and formation. *Wood science and technology*, 10(1):1–8, 1976.
- R. M. Burns, B. H. Honkala, et al. Silvics of north america. volume 1. conifers. *Agriculture Handbook (Washington)*, 1(654), 1990.
- D. J. Chmura and M. G. Tjoelker. Leaf traits in relation to crown development, light interception and growth of elite families of loblolly and slash pine. *Tree Physiology*, 28(5):729–742, 2008.
- D. J. Chmura, M. S. Rahman, and M. G. Tjoelker. Crown structure and biomass allocation patterns modulate aboveground productivity in young loblolly pine and slash pine. *Forest ecology and management*, 243(2-3):219–230, 2007.
- M. Fagan, D. Morton, B. Cook, J. Masek, F. Zhao, R. Nelson, and C. Huang. Mapping pine plantations in the southeastern us using structural, spectral, and temporal remote sensing data. *Remote sensing of environment*, 216:415–426, 2018.
- L. I. Gaby. Southern pines: loblolly pine (*Pinus taeda* l.), longleaf pine (*Pinus palustris* mill.), shortleaf pine (*Pinus echinata* mill.), slash pine (*Pinus elliottii* engelm.). *FS-256*, 256, 1985.
- C. A. Gonzalez-Benecke, S. A. Gezan, T. J. Albaugh, H. L. Allen, H. E. Burkhart, T. R. Fox, E. J. Jokela, C. A. Maier, T. A. Martin, R. A. Rubilar, and L. J. Samuelson. Local and general above-stump biomass functions for loblolly pine and slash pine trees. *Forest Ecology and Management*, 334:254–276, 2014. ISSN 0378-1127.
- B. Huber. *Weitere quantitative Untersuchungen über das Wasserleitungssystem der Pflanzen*. Jahrb Wiss Bot, 1928.
- W.-T. Jin, D. S. Gernandt, C. Wehenkel, X.-M. Xia, X.-X. Wei, and X.-Q. Wang. Phylogenomic and ecological analyses reveal the spatiotemporal evolution of global pines. *Proceedings of the National Academy of Sciences*, 118(20), 2021.
- J. E. Keeley. Ecology and evolution of pine life histories. *Annals of Forest Science*, 69(4):445–453, 2012.

- R. Lehnebach, R. Beyer, V. Letort, and P. Heuret. The pipe model theory half a century on: a review. *Annals of botany*, 121(5):773–795, 2018.
- C. A. Maier, K. H. Johnsen, P. H. Anderson, S. Palmroth, D. Kim, H. R. McCarthy, and R. Oren. The response of coarse root biomass to long-term co₂ enrichment and nitrogen application in a maturing *pinus taeda* stand with a large broadleaved component. *Global change biology*, 2021.
- MATLAB. *version 9.9.0 (R2020b)*. The MathWorks Inc., Natick, Massachusetts, 2020.
- N. McDowell, H. Barnard, B. Bond, T. Hinckley, R. Hubbard, H. Ishii, B. Köstner, F. Magnani, J. Marshall, F. Meinzer, et al. The relationship between tree height and leaf area: sapwood area ratio. *Oecologia*, 132(1):12–20, 2002.
- R. Oren, K. S. Werk, and E.-D. Schulze. Relationships between foliage and conducting xylem in *Picea abies* (L.) karst. *Trees*, 1:61–69, 1986.
- L. J. Samuelson, T. A. Stokes, and K. H. Johnsen. Ecophysiological comparison of 50-year-old longleaf pine, slash pine and loblolly pine. *Forest ecology and management*, 274:108–115, 2012.
- K. Shinozaki, K. Yoda, K. Hozumi, and T. Kira. A quantitative analysis of plant form-the pipe model theory: I. basic analyses. *Japanese Journal of ecology*, 14(3):97–105, 1964a.
- K. Shinozaki, K. Yoda, K. Hozumi, and T. Kira. A quantitative analysis of plant form-the pipe model theory: II. further evidence of the theory and its application in forest ecology. *Japanese journal of ecology*, 14(4):133–139, 1964b.
- S. C. Stearns-Smith, E. J. Jokela, and R. C. Abt. Thinning and fertilizing southern pine stands of the lower coastal plain: biological and economic effects. *Southern Journal of Applied Forestry*, 16(4):186–193, 1992.
- M. Thérézien, S. Palmroth, R. Brady, and R. Oren. Estimation of light interception properties of conifer shoots by an improved photographic method and a 3d model of shoot structure. *Tree physiology*, 27(10):1375–1387, 2007.

- N. Wang, S. Palmroth, C. A. Maier, J.-C. Domec, and R. Oren. Anatomical changes with needle length are correlated with leaf structural and physiological traits across five *Pinus* species. *Plant, Cell & Environment*, 42(5):1690–1704, 2019.
- R. Waring, P. Schroeder, and R. Oren. Application of the pipe model theory to predict canopy leaf area. *Canadian Journal of Forest Research*, 12(3):556–560, 1982.
- R. H. Waring. Estimating forest growth and efficiency in relation to canopy leaf area. *Advances in ecological research*, 13:327–354, 1983.
- D. N. Wear and J. G. Greis. Southern forest resource assessment: summary of findings. *Journal of Forestry*, 100(7):6–14, 2002.
- D. N. Wear and J. G. Greis. The southern forest futures project: summary report. *Gen. Tech. Rep. SRS-GTR-168*. Asheville, NC: USDA-Forest Service, Southern Research Station. 54 p., 168:1–54, 2012.

Appendix

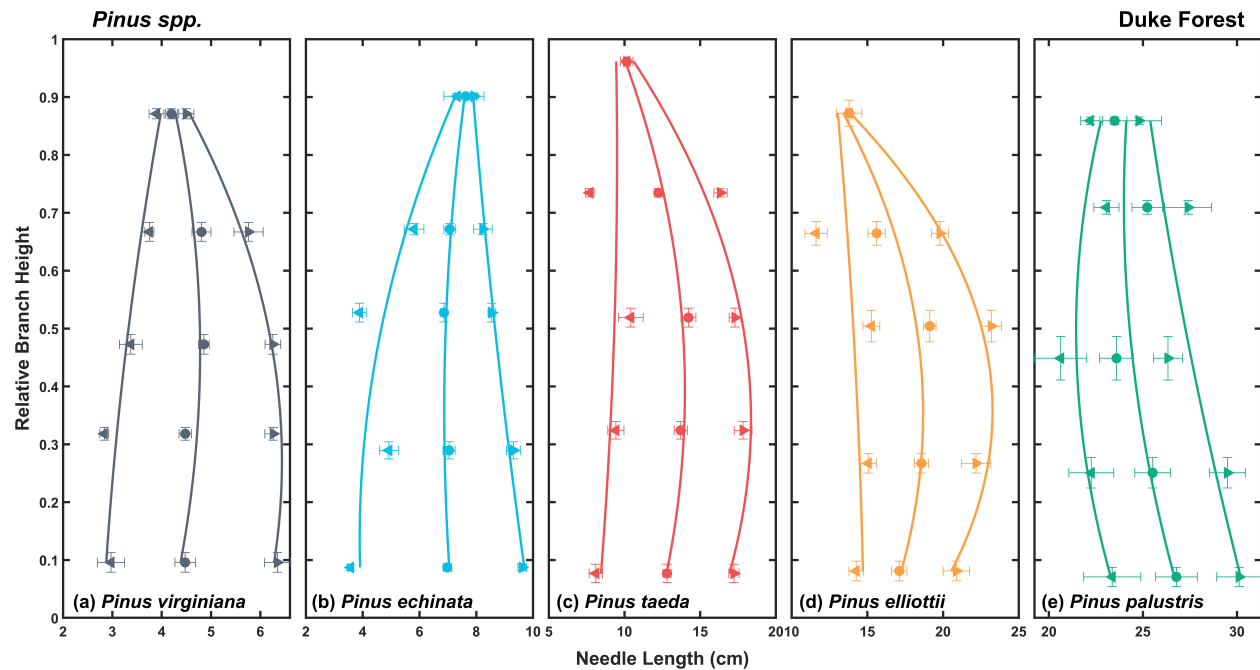


Figure S1: Relationships between needle length and relative branch height within the crown of five *Pinus* species. Round points represent species means of average needle length at each live crown section and error bars represent standard errors of the means ($n = 5$). Left pointing and right pointing triangles represent species means of minimum and maximum needle length at each live crown section and error bars represent standard errors of the means ($n = 5$), respectively. Lines represent the fits from Modified Akima piecewise cubic Hermite interpolation. Lines are intended to guide the eye only.

Table S1: Coefficient estimates and fit statistics of above-ground biomass allometric equation in five *Pinus* species ($y = a(DBH^2 * Height)^b$)

Species	Code	DBH (cm)	Height (m)	a	SE	b	SE	R ²	RMSE
<i>Pinus virginiana</i>	PV	3.2 - 10.2	2.65 - 5.56	0.084449	0.046696	0.90075	0.08992	0.990947	0.999426
<i>Pinus echinata</i>	PEC	5.5 - 11.3	3.31 - 5.67	0.130476	0.064437	0.760464	0.077823	0.980511	0.964053
<i>Pinus taeda</i>	PT	11.1 - 15.9	7.80 - 10.90	0.010681	0.003999	1.068585	0.048366	0.993983	1.113774
<i>Pinus elliottii</i>	PEL	8.1 - 11.5	4.95 - 7.09	0.005196	0.006273	1.253546	0.182608	0.930974	2.219962
<i>Pinus palustris</i>	PP	6.3 - 16.3	4.28 - 8.51	0.076894	0.010138	0.84117	0.017629	0.99928	0.529983

Table S2: Coefficient estimates and fit statistics of below-ground biomass allometric equation in five *Pinus* species ($y = a(DBH^2 * Height)^b$)

Species	Code	DBH (cm)	Height (m)	a	SE	b	SE	R ²	RMSE
<i>Pinus virginiana</i>	PV	3.2 - 10.2	2.65 - 5.56	0.048278	0.039666	0.788525	0.134079	0.972018	0.501201
<i>Pinus echinata</i>	PEC	5.5 - 11.3	3.31 - 5.67	0.178316	0.168554	0.546759	0.150959	0.841653	0.844838
<i>Pinus taeda</i>	PT	11.1 - 15.9	7.80 - 10.90	0.053407	0.120143	0.669834	0.293351	0.536193	1.82786
<i>Pinus elliottii</i>	PEL	8.1 - 11.5	4.95 - 7.09	0.001128	0.00175	1.25032	0.234682	0.894936	0.607015
<i>Pinus palustris</i>	PP	6.3 - 16.3	4.28 - 8.51	0.051464	0.025465	0.731677	0.066585	0.984666	0.682531

Table S3: Coefficient estimates and fit statistics of stem biomass allometric equation in five *Pinus* species ($y = a(DBH^2 * Height)^b$)

Species	Code	DBH (cm)	Height (m)	a	SE	b	SE	R ²	RMSE
<i>Pinus virginiana</i>	PV	3.2 - 10.2	2.65 - 5.56	0.020664	0.011261	0.989656	0.088431	0.992976	0.374366
<i>Pinus echinata</i>	PEC	5.5 - 11.3	3.31 - 5.67	0.03361	0.008385	0.892562	0.039099	0.996762	0.248839
<i>Pinus taeda</i>	PT	11.1 - 15.9	7.80 - 10.90	0.02265	0.006723	0.924037	0.038462	0.99465	0.653456
<i>Pinus elliottii</i>	PEL	8.1 - 11.5	4.95 - 7.09	0.007875	0.004478	1.109359	0.086432	0.97918	0.649798
<i>Pinus palustris</i>	PP	6.3 - 16.3	4.28 - 8.51	0.03788	0.010902	0.867512	0.038432	0.996901	0.670554

Table S4: Coefficient estimates and fit statistics of branch biomass allometric equation in five *Pinus* species ($y = aDBH^b$)

Species	Code	DBH (cm)	Height (m)	a	SE	b	SE	R ²	RMSE
<i>Pinus virginiana</i>	PV	3.2 - 10.2	2.65 - 5.56	0.042652	0.023368	2.332160	0.244249	0.991016	0.378871
<i>Pinus echinata</i>	PEC	5.5 - 11.3	3.31 - 5.67	0.028085	0.056757	2.051435	0.857406	0.751219	0.852459
<i>Pinus taeda</i>	PT	11.1 - 15.9	7.80 - 10.90	0.000087	0.000077	4.199993	0.326951	0.986113	0.413672
<i>Pinus elliottii</i>	PEL	8.1 - 11.5	4.95 - 7.09	0.000006	0.000018	5.575985	1.246392	0.880175	0.624960
<i>Pinus palustris</i>	PP	6.3 - 16.3	4.28 - 8.51	0.001429	0.000448	3.197780	0.114815	0.998373	0.177475

Table S5: Coefficient estimates and fit statistics of foliage biomass allometric equation in five *Pinus* species ($y = a(DBH^2 * Height)^b$)

Species	Code	DBH (cm)	Height (m)	a	SE	b	SE	R ²	RMSE
<i>Pinus virginiana</i>	PV	3.2 - 10.2	2.65 - 5.56	0.020265	0.020911	0.864361	0.167995	0.962624	0.375980
<i>Pinus echinata</i>	PEC	5.5 - 11.3	3.31 - 5.67	0.113416	0.144781	0.517571	0.204355	0.699446	0.625503
<i>Pinus taeda</i>	PT	11.1 - 15.9	7.80 - 10.90	0.000455	0.000520	1.213700	0.147017	0.959982	0.416152
<i>Pinus elliottii</i>	PEL	8.1 - 11.5	4.95 - 7.09	0.000952	0.002268	1.302605	0.360019	0.772266	1.086867
<i>Pinus palustris</i>	PP	6.3 - 16.3	4.28 - 8.51	0.128791	0.054293	0.561746	0.057552	0.975917	0.527449

Table S6: Coefficient estimates and fit statistics of linear regression model between DBH and foliage biomass percentage in five *Pinus* species ($y = a + b * DBH$)

Species	Code	DBH (cm)	a	b	R ²	p
<i>Pinus virginiana</i>	PV	3.2 - 10.2	24.64	-1.07	0.81	0.0372
<i>Pinus echinata</i>	PEC	5.5 - 11.3	25.48	-1.12	0.61	0.1185
<i>Pinus taeda</i>	PT	11.1 - 15.9	5.23	0.36	0.81	0.0371
<i>Pinus elliottii</i>	PEL	8.1 - 11.5	30.83	-1.02	0.20	0.4536
<i>Pinus palustris</i>	PP	6.3 - 16.3	33.12	-1.13	0.73	0.0654

Table S7: Coefficient estimates and fit statistics of linear regression model between DBH and branch biomass percentage in five *Pinus* species ($y = a + b * DBH$)

Species	Code	DBH (cm)	a	b	R ²	p
<i>Pinus virginiana</i>	PV	3.2 - 10.2	18.52	1.10	0.77	0.0523
<i>Pinus echinata</i>	PEC	5.5 - 11.3	7.82	0.79	0.30	0.3434
<i>Pinus taeda</i>	PT	11.1 - 15.9	-5.50	1.32	0.85	0.0271
<i>Pinus elliottii</i>	PEL	8.1 - 11.5	0.85	1.13	0.33	0.3082
<i>Pinus palustris</i>	PP	6.3 - 16.3	-1.98	1.13	0.97	0.0024

Table S8: Coefficient estimates and fit statistics of linear regression model between DBH and stem biomass percentage in five *Pinus* species ($y = a + b * DBH$)

Species	Code	DBH (cm)	a	b	R ²	p
<i>Pinus virginiana</i>	PV	3.2 - 10.2	36.82	-0.46	0.16	0.4996
<i>Pinus echinata</i>	PEC	5.5 - 11.3	28.81	1.41	0.48	0.1971
<i>Pinus taeda</i>	PT	11.1 - 15.9	67.27	-0.74	0.12	0.5720
<i>Pinus elliottii</i>	PEL	8.1 - 11.5	58.67	-0.89	0.13	0.5507
<i>Pinus palustris</i>	PP	6.3 - 16.3	38.19	0.54	0.59	0.1275

Table S9: Coefficient estimates and fit statistics of linear regression model between DBH and taproot biomass percentage in five *Pinus* species ($y = a + b * DBH$)

Species	Code	DBH (cm)	a	b	R ²	p
<i>Pinus virginiana</i>	PV	3.2 - 10.2	5.60	-0.07	0.07	0.6590
<i>Pinus echinata</i>	PEC	5.5 - 11.3	8.05	-0.08	0.01	0.8549
<i>Pinus taeda</i>	PT	11.1 - 15.9	13.43	-0.30	0.35	0.2967
<i>Pinus elliottii</i>	PEL	8.1 - 11.5	4.16	0.29	0.20	0.4479
<i>Pinus palustris</i>	PP	6.3 - 16.3	8.19	-0.04	0.01	0.8568

Table S10: Coefficient estimates and fit statistics of linear regression model between DBH and lateral root biomass percentage in five *Pinus* species ($y = a + b * DBH$)

Species	Code	DBH (cm)	a	b	R ²	p
<i>Pinus virginiana</i>	PV	3.2 - 10.2	14.84	0.30	0.28	0.3635
<i>Pinus echinata</i>	PEC	5.5 - 11.3	29.93	-1.02	0.60	0.1257
<i>Pinus taeda</i>	PT	11.1 - 15.9	19.57	-0.64	0.17	0.4942
<i>Pinus elliottii</i>	PEL	8.1 - 11.5	5.49	0.49	0.16	0.5055
<i>Pinus palustris</i>	PP	6.3 - 16.3	22.50	-0.50	0.51	0.1779

Table S11: Coefficient estimates and fit statistics of linear regression model between DBH and total root biomass percentage in five *Pinus* species ($y = a + b * DBH$)

Species	Code	DBH (cm)	a	b	R ²	p
<i>Pinus virginiana</i>	PV	3.2 - 10.2	20.44	0.23	0.20	0.4485
<i>Pinus echinata</i>	PEC	5.5 - 11.3	37.98	-1.10	0.36	0.2864
<i>Pinus taeda</i>	PT	11.1 - 15.9	33.00	-0.95	0.21	0.4345
<i>Pinus elliottii</i>	PEL	8.1 - 11.5	9.65	0.78	0.18	0.4707
<i>Pinus palustris</i>	PP	6.3 - 16.3	30.68	-0.54	0.71	0.0745

Table S12: Coefficient estimates and fit statistics of linear regression model between branch sapwood area and branch leaf area in five *Pinus* species (Leaf area = a * Sapwood area)

Species	Code	a	R ²	RMSE	p
<i>Pinus virginiana</i>	PV	0.11	0.75	0.08	< 0.0001
<i>Pinus echinata</i>	PEC	0.14	0.63	0.11	< 0.0001
<i>Pinus taeda</i>	PT	0.20	0.83	0.16	< 0.0001
<i>Pinus elliottii</i>	PEL	0.22	0.82	0.13	< 0.0001
<i>Pinus palustris</i>	PP	0.18	0.93	0.09	< 0.0001

Table S13: Coefficient estimates and fit statistics of linear regression model between branch sapwood area and branch leaf mass in five *Pinus* species (Leaf mass = a * Sapwood area)

Species	Code	a	R ²	RMSE	p
<i>Pinus virginiana</i>	PV	0.03	0.78	0.02	< 0.0001
<i>Pinus echinata</i>	PEC	0.03	0.61	0.03	< 0.0001
<i>Pinus taeda</i>	PT	0.04	0.81	0.03	< 0.0001
<i>Pinus elliottii</i>	PEL	0.06	0.81	0.04	< 0.0001
<i>Pinus palustris</i>	PP	0.05	0.95	0.03	< 0.0001

Table S14: Coefficient estimates and fit statistics of linear regression model between sapwood area at base of live crown and total leaf area in five *Pinus* species (Leaf area = a + b * Crown base sapwood area)

Species	Code	a	b	R ²	RMSE	p
<i>Pinus virginiana</i>	PV	-0.53	0.22	0.87	2.57	0.0139
<i>Pinus echinata</i>	PEC	3.09	0.13	0.60	2.81	0.0775
<i>Pinus taeda</i>	PT	-5.92	0.27	0.93	2.68	0.0047
<i>Pinus elliottii</i>	PEL	1.79	0.17	0.02	7.40	0.3732
<i>Pinus palustris</i>	PP	2.21	0.21	0.89	4.31	0.0104
<i>All</i>	All	-0.50	0.22	0.83	3.97	< 0.0001

Table S15: Coefficient estimates and fit statistics of linear regression model between sapwood area at base of live crown and total leaf mass in five *Pinus* species (Leaf mass = a + b * Crown base sapwood area)

Species	Code	a	b	R ²	RMSE	p
<i>Pinus virginiana</i>	PV	-0.29	0.06	0.90	0.61	0.0086
<i>Pinus echinata</i>	PEC	0.75	0.03	0.48	0.83	0.1203
<i>Pinus taeda</i>	PT	-0.78	0.05	0.93	0.53	0.0047
<i>Pinus elliottii</i>	PEL	0.61	0.05	-0.01	2.29	0.4009
<i>Pinus palustris</i>	PP	0.85	0.06	0.88	1.18	0.0118
<i>All</i>	All	0.16	0.05	0.73	1.24	< 0.0001

Table S16: Coefficient estimates and fit statistics of linear regression model between sapwood area at base of live crown and total branch sapwood area in five *Pinus* species (Total branch sapwood area = a + b * Crown base sapwood area)

Species	Code	a	b	R ²	RMSE	p
<i>Pinus virginiana</i>	PV	5.02	1.94	0.96	11.89	0.0022
<i>Pinus echinata</i>	PEC	11.03	1.16	0.81	15.05	0.0234
<i>Pinus taeda</i>	PT	-16.88	1.47	0.86	22.36	0.0150
<i>Pinus elliottii</i>	PEL	4.93	1.10	0.00	50.68	0.3903
<i>Pinus palustris</i>	PP	-9.76	1.59	0.96	17.69	0.0018
<i>All</i>	All	2.78	1.39	0.78	29.21	< 0.0001